Smoking-associated inflammation: A dual ^{18}F-FDG PET/CT analysis of tonsillar and aortic inflammation using liver-normalized SUVmax

Emmanouil Panagiotidis[1,2] MD, PhD,
George Angelidis[1] MD, PhD,
Anna Paschali[2] MD, PhD,
Theodoros Kalathas[2] MD, PhD,
Varvara Valotassiou[1] MD, PhD,
Vasiliki Chatzipavlidou[2] MD, PhD,
Panagiotis Georgoulias[1] MD, PhD

1. Nuclear Medicine Laboratory, University of Thessaly, University Hospital of Larissa, Larissa, Greece.
2. Department of Nuclear Medicine, Theageneio Anticancer Centre, Thessaloniki, Greece.

Keywords: ^{18}F-FDG - Aortic inflammation - Tonsillar inflammation - Smoking

Corresponding author:
George Angelidis MD, PhD
Nuclear Medicine Laboratory, University of Thessaly, University Hospital of Larissa, GR 41110, Mezourlo, Larissa, Greece.
Tel: +30 241350 2916
angelidis@protonmail.ch

Received:
26 April 2026
Accepted revised:
30 June 2026

Abstract

Objective: Cigarette smoking alters immune and vascular systems, yet its dual inflammatory impact on mucosal lymphoid tissues and arterial walls remains underexplored in vivo. This study employs fluorine-18-fluorodeoxyglucose (^{18}F-FDG) positron emission tomography/computed tomography (PET/CT) with liver-normalized maximum standardized uptake value (SUVmax) to assess metabolic inflammation in Waldeyer's ring and the thoracic aorta across smoking groups. **Subjects and Methods:** We retrospectively analyzed ^{18}F-FDG PET/CT scans from 222 patients categorized by smoking status. Maximum SUV was recorded in the palatine, lingual, and nasopharyngeal tonsils and the thoracic aorta. Values were normalized to liver uptake. Group differences were analyzed using Kruskal-Wallis tests with Bonferroni-corrected Mann-Whitney post hoc comparisons. Pearson correlation assessed associations with cigarette consumption. **Results:** Smokers had slightly reduced tonsillar SUVmax values, especially in the lingual tonsil (mean 3.56 vs. 3.82 in non-smokers), but these differences were not statistically significant after liver normalization. In contrast, raw aortic SUVmax was highest in non-smokers (2.72), but after normalization, ex-smokers demonstrated significantly elevated aortic uptake (P=0.016). No significant associations were observed between cigarette quantity and regional SUV values, possibly due to individual variability and confounding metabolic factors such as body mass index (BMI). **Conclusions:** Fluorine-18-FDG PET/CT reveals mild immune suppression in tonsillar lymphoid tissue among smokers and persistent vascular inflammation in ex-smokers. Liver normalization is essential for identifying true inflammatory differences in metabolically heterogeneous populations. These findings suggest that inflammation is a multiparametric process influenced by factors such as BMI and metabolic status, which may mask smoking-related effects unless properly adjusted for.

Hell J Nucl Med 2026; 29(2): 64-69 *Epub ahead of print: 6 August 2026* *Published online: 31 August 2026*

Introduction

Cigarette smoking remains a global health burden, responsible for over 8 million deaths annually and implicated in cardiovascular disease, cancer, and immune dysfunction [1]. Its dual impact on mucosal immunity and vascular inflammation is well-documented but rarely examined simultaneously in vivo.

Waldeyer's ring - including palatine, lingual, and nasopharyngeal tonsils - serves as a critical mucosal immune barrier. Chronic tobacco exposure impairs lymphoid architecture, suppresses antigen presentation, and alters cytokine signaling [2, 3]. Vascularly, tobacco promotes endothelial dysfunction, leukocyte infiltration, and macrophage activation - key hallmarks of atherosclerosis [4]. This inflammatory cascade within the vessel wall, driven by immune cell infiltration, is now recognized as a central mechanism in the development and progression of atherosclerotic plaques [4]. This regional disparity in immune and vascular responses may be better understood through a combined imaging approach. Furthermore, this smoking-induced vascular damage is often compounded by underlying metabolic dysfunction, such as that seen in metabolic syndrome, which is itself characterized by a state of chronic, low-grade inflammation [5].

Fluorine-18-fluorodeoxyglucose (^{18}F-FDG) positron emission tomography/computed tomography (PET/CT) offers a validated, non-invasive method to assess inflammation by visualizing tissue glucose metabolism [6-8]. Fluorine-18-FDG uptake has been used to assess both immune activation in lymphoid organs and vascular inflammation in atherosclerotic plaques. However, prior studies have largely addressed these targets independently. This study addresses that gap by evaluating ^{18}F-FDG uptake in both Waldeyer's

ring and thoracic aorta within the same cohort.

Normalization to liver maximum standardized uptake value (SUVmax) is an important methodological tool, minimizing inter-subject variability linked to systemic factors such as obesity, hepatic steatosis, and glycemic state [5, 9]. Here, we compare both raw and normalized SUVmax values, aiming to assess the impact of smoking and cessation on regional inflammation.

Recent literature supports the use of ^{18}F-FDG PET/CT to detect inflammation in vascular and systemic disorders. Fluorine-18-FDG uptake has been validated as a surrogate for inflammatory activity in both large-vessel vasculitis and atherosclerotic disease [8, 10, 11].

Furthermore, studies suggest that persistent aortic ^{18}F-FDG uptake is predictive of future cardiovascular events and reflects active atherosclerotic inflammation [9, 10]. Additionally, ^{18}F-FDG uptake in the aortic wall has been proposed as a marker of active atherosclerosis, even in asymptomatic individuals, highlighting its potential role in early vascular inflammation detection [12]. These findings reinforce our rationale: dual-site imaging combined with normalization improves detection of subtle inflammatory patterns unique to smoking status.

Subjects and Methods

Study design and population

This retrospective study included 222 adult patients who underwent clinically indicated whole-body ^{18}F-FDG PET/CT between January 2022 and January 2025 from two tertiary hospitals: Theageneio Cancer Center (n=79) and the University Hospital of Larissa (n=143). Ethical approval for anonymized data analysis was obtained from the institutional review boards of both centers.

Inclusion criteria: age ≥18 years; adequate documentation of smoking history; clinically indicated ^{18}F-FDG PET/CT (oncologic, inflammatory, or surveillance); no major anatomical distortion of target regions.

Exclusion criteria: prior neck radiotherapy or tonsillectomy; head and neck or mediastinal malignancy; acute infection within 4 weeks prior to scanning; incomplete or unreliable smoking history; poor PET/CT image quality or misregistration artifacts.

Patients were categorized into three groups based on smoking status: non-smokers (n=60), lifetime cigarette consumption fewer than 100 cigarettes; current smokers (n=103), actively smoking daily at the time of PET/CT; and ex-smokers (n=59), abstinent from smoking for more than 6 months prior to scanning. Clinical and demographic data collected included age, sex, body mass index (BMI), systolic and diastolic blood pressure, glucose levels at scan time, and cigarettes per day.

PET/CT acquisition protocol

All patients fasted for at least 6 hours before imaging, following standard European Association of Nuclear Medicine (EANM) guidelines [13]. Blood glucose was measured upon patient arrival, and scans proceeded only if glucose levels were below 200mg/dL, unless clinically justified. Patients received 3.7MBq/kg of ^{18}F-FDG intravenously, followed by a 60-minute uptake period in a controlled, restful environment.

Positron emission tomography/CT imaging was conducted using GE Discovery 690 and 710 systems (GE Healthcare), each equipped with time-of-flight and point spread function correction. Initially, CT imaging (120kVp, auto mA, slice thickness 3.75mm) was performed for attenuation correction and anatomical localization, immediately followed by PET emission imaging from the skull vertex to mid-thigh, at 2-3 minutes per bed position. Positron emission tomography images were reconstructed using iterative ordered-subset expectation maximization (OSEM), 2 iterations, 24 subsets, and a Gaussian filter of 6.4mm.

Region of interest (ROI) definition

All PET/CT measurements were performed by a board-certified nuclear medicine physician (18 years of experience), blinded to patient history and group assignments. Images were reviewed using GE Advantage Workstation software (version 4.7, GE Healthcare).

Maximum SUV were measured within spherical 3D regions of interest (10-12mm diameter) placed on: palatine tonsils (right and left); lingual tonsil (posterior tongue base); nasopharyngeal tonsil (adenoid area); thoracic aorta (aortic arch level); and liver (right lobe segment VIII, for normalization). Care was taken to avoid adjacent hypermetabolic tissue and partial-volume artifacts. Maximum SUV normalization was performed by dividing each region's SUVmax by the corresponding liver SUVmax, consistent with standard practice for reducing inter-individual metabolic variability [13, 14].

Normalization calculation

$$\text{Normalized SUVmax} = \frac{\text{Region SUVmax}}{\text{Liver SUVmax}}$$

Statistical analysis

Statistical analyses were conducted using SPSS (version 27, IBM Corp., Armonk, NY). Continuous variables were reported as means±standard deviation or medians (interquartile range). Group differences in raw and liver-normalized SUVmax values were evaluated using the Kruskal-Wallis test, followed by Bonferroni-adjusted Mann-Whitney U post hoc tests for pairwise comparisons.

Pearson correlation coefficients assessed the relationship between SUVmax and daily cigarette consumption. Statistical significance was set at $P<0.05$ (two-sided).

Results were summarized in tables showing mean SUVmax values (raw and normalized), intergroup comparisons, and correlations. Visualization included boxplots for raw and normalized aortic SUVmax.

Results

Patient characteristics

A total of 222 patients were included in the analysis, distributed as follows: non-smokers, n=60; current smokers, n=103; ex-smokers, n=59. The mean age of the cohort was 64.2±9.5 years. Non-smokers had the highest average BMI (29.98±3.7kg/m^2), followed by smokers (28.34±4.1kg/m^2) and ex-smokers (27.15±4.0kg/m^2). Smokers and ex-smokers reported similar cigarette consumption, averaging 25.6±8.3 and 25.4±7.6 cigarettes per day, respectively.

Regional ^{18}F-FDG uptake: raw and liver-normalized SUVmax

Mean SUVmax values (raw and normalized to liver) for each anatomical region and group are summarized in Table 1. Among tonsillar structures, smokers had slightly lower SUVmax in the lingual tonsil compared to non-smokers (3.56 vs. 3.82), but this was not statistically significant. Nasopharyngeal SUVmax showed the only regionally significant group difference in uncorrected values (P=0.020, Kruskal-Wallis), though this did not persist after normalization.

Post hoc comparisons of raw SUVmax

Post hoc testing (Bonferroni-adjusted Mann-Whitney U) of raw SUVmax values between groups is shown in Table 2. No statistically significant differences were found in the tonsillar regions between any groups. However, aortic SUVmax in ex-smokers vs. non-smokers reached significance (P=0.016).

Correlation with cigarette consumption

Pearson correlation analysis of SUVmax versus daily cigarette consumption revealed no strong linear relationships in any region. Correlation coefficients (r) ranged from -0.10 (right palatine) to +0.07 (aorta normalized), with no P-values reaching statistical significance.

Visualization of aortic SUVmax by smoking group

A boxplot (see Figure 1) clearly demonstrates the difference in thoracic aortic SUVmax between groups. In raw values, non-smokers appeared to show the highest uptake. However, after normalization to liver SUV, ex-smokers exhibited the highest median aortic SUV, suggesting subclinical vascular inflammation that was otherwise obscured.

Discussion

This study used ^{18}F-FDG PET/CT to assess inflammation in both lymphoid and vascular tissues in smokers, ex-smokers, and non-smokers. Two key findings emerged: (1) modest suppression of immune activity in Waldeyer's ring among active smokers, and (2) persistent vascular inflammation in ex-smokers that became evident only after normalizing aortic SUVmax to liver uptake.

The lower ^{18}F-FDG uptake observed in the lingual tonsil of current smokers supports previous histological data indicating that tobacco use leads to mucosal lymphoid atrophy and decreased immune cell density in the upper airway [2]. Although not statistically significant after normalization, this trend reflects the immunosuppressive effects of chronic smoking on mucosal immune function, possibly due to impaired dendritic cell activation and altered lymphocyte trafficking [15]. These effects contribute to the increased susceptibility of smokers to upper respiratory infections and may compromise mucosal antigen surveillance [2, 15].

Table 1. *Raw and liver-normalized SUVmax by smoking group.*

Group	Rt Pal (Raw)	Lt Pal (Raw)	Lingual (Raw)	Naso (Raw)	Aorta (Raw)	Rt Pal (Norm)	Lt Pal (Norm)	Lingual (Norm)	Naso (Norm)	Aorta (Norm)
Non-smokers	4.33	4.51	3.82	3.96	2.72	1.22	1.27	1.08	1.12	0.76
Smokers	4.42	4.40	3.56	4.06	2.55	1.35	1.34	1.09	1.24	0.77
Ex-smokers	4.32	4.29	3.61	4.05	2.52	1.39	1.39	1.17	1.31	0.80

Rt Pal, right palatine tonsil; Lt Pal, left palatine tonsil; Naso, nasopharyngeal tonsil; Raw, unadjusted SUVmax; Norm, liver-normalized SUVmax.

Table 2. *Post hoc comparisons (Bonferroni-adjusted P-values).*

Region	NS vs Smokers	NS vs Ex-smokers	Smokers vs Ex-smokers
Right palatine	1.000	1.000	1.000
Left palatine	1.000	1.000	1.000
Lingual	0.594	0.972	1.000
Nasopharyngeal	1.000	1.000	1.000
Aorta	0.055	0.016	1.000

NS, non-smokers.

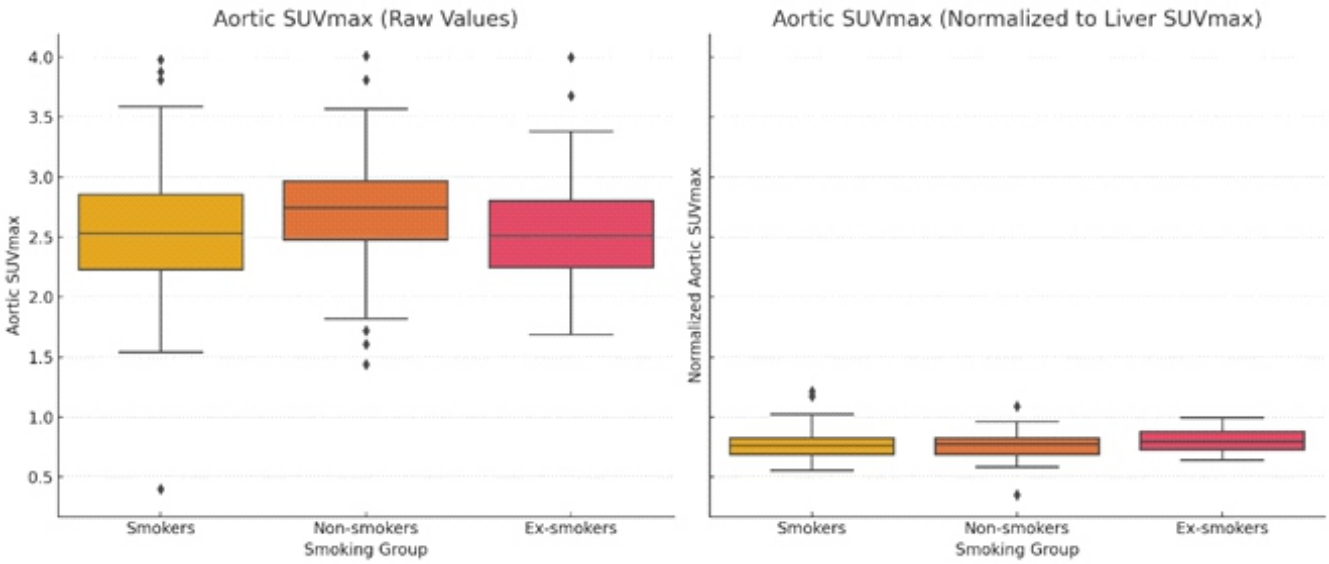

Figure 2. Transition line graphs showing changes in (a) harmonized SUVmax, (b) harmonized SUVpeak, (c) harmonized SUVmean, (d) harmonized MBV, and (e) harmonized TBU between the first and second SPECT/CT examinations in the 23 responder lesions.

However, the use of Bonferroni correction, while effective at minimizing false positives, may have been overly conservative, increasing the risk of Type II error and potentially obscuring subtle but clinically relevant differences - such as the near-significant aortic inflammation observed between current and non-smokers. Furthermore, the non-smoker group exhibited a notably higher average BMI (29.98) compared to the smoker groups. Given that elevated BMI is a recognized driver of systemic inflammation and increased ^{18}F-FDG uptake, this likely explains the unexpectedly high raw aortic SUVmax in non-smokers. While liver normalization mitigates this confounding, the impact of BMI on unadjusted values should be carefully considered when interpreting results.

In contrast, vascular ^{18}F-FDG uptake patterns required careful interpretation. While uncorrected SUVmax values were highest in non-smokers, liver-normalized values revealed significantly greater aortic activity in ex-smokers. This highlights the importance of liver normalization in studies of vascular inflammation, especially in populations with variable metabolic states, such as obesity or insulin resistance [5]. Without normalization, underlying arterial inflammation may be underestimated due to inter-individual differences in hepatic ^{18}F-FDG metabolism [5, 14].

The elevated aortic ^{18}F-FDG uptake in ex-smokers is particularly noteworthy, as it may reflect a prolonged inflammatory response in the vascular wall that persists even after cessation of smoking. This is consistent with findings by Rudd et al. (2002) and Tawakol et al. (2006), who demonstrated that ^{18}F-FDG uptake corresponds to macrophage-rich atherosclerotic plaques and active inflammation [8, 11].

Moreover, ex-smokers may retain a pro-inflammatory vascular phenotype due to epigenetic modifications and residual oxidative stress [4]. Supporting this notion, Coulson et al. (2010) reported significantly elevated aortic ^{18}F-FDG uptake in ex-smokers with chronic obstructive pulmonary disease (CO PD), underscoring the durability of tobacco-induced vascular inflammation [17]. In parallel, Torigian et al. (2017) demonstrated that chronic tobacco use leads to systemic metabolic alterations detectable by ^{18}F-FDG PET/CT, reinforcing the view that inflammation may not be limited to individual vascular beds but represents a broader immune-metabolic dysregulation [18]. These findings imply that even after cessation, vascular inflammation may persist due to chronic im-mune activation or irreversible endothelial changes. This reinforces the clinical utility of ^{18}F-FDG PET/CT in identifying residual inflammatory risk and supports its role in guiding secondary prevention strategies [9, 10].

The absence of significant differences in raw ^{18}F-FDG uptake between current and ex-smokers - particularly in lymphoid regions - may reflect the multifactorial nature of systemic inflammation. Fluorine-18-FDG uptake is modulated by several variables including BMI, insulin sensitivity, hepatic steatosis, and overall metabolic activity, all of which can affect both background liver SUV and regional tissue metabolism. These results underscore that inflammation is not driven by a single factor such as tobacco exposure alone, but reflects a complex interplay of metabolic, genetic, and immune variables. The absence of a uniform ^{18}F-FDG increase across all regions or smoking categories underscores the multifactorial and heterogeneous nature of inflammation, influenced by both environmental exposure and individual metabolic status.

This metabolic heterogeneity may obscure inflammation differences attributable solely to smoking status. As such, smoking-related immune suppression and vascular inflammation likely interact with these host-specific parameters, supporting the rationale for liver normalization and for interpreting PET findings within a broader clinical context [5, 14].

Importantly, no significant correlations were found between cumulative tobacco exposure (pack-years) and ^{18}F-FDG uptake in either region. This suggests a possible threshold effect or inter-individual variation in inflammatory res-

ponse to tobacco exposure [4, 10]. These findings align with the understanding that atherosclerotic inflammation is a complex interplay between environmental risk factors and host immune responses [4, 19, 20].

The methodological importance of SUV normalization was reinforced by this study. Liver-corrected aortic SUVmax values provided clearer differentiation between groups, in line with EANM procedural guidance [13, 14]. Liver normalization has been validated as a method to reduce variability in PET-derived inflammation metrics, especially when evaluating vascular territories in heterogeneous populations [16, 21].

From a clinical perspective, this dual-region protocol combining assessment of mucosal immune function and vascular inflammation may be valuable in evaluating systemic immune activity. Persistent aortic inflammation in ex-smokers could help identify individuals at heightened cardiovascular risk, even after cessation, and support further evaluation with biomarkers such as high-sensitivity C-reactive protein (hsCRP) or interleukin-6 (IL-6) [9].

Limitations of this study include its retrospective design, the absence of serum inflammatory biomarkers, and the lack of dynamic PET acquisition. The group sizes were also unbalanced (non-smokers: 60, current smokers: 103, ex-smokers: 59), which is common in retrospective analyses but may reduce the statistical power to detect differences, particularly in the smaller groups. Nonetheless, the standardized imaging protocol with consistent 60-minute post-injection timing adheres to current guidelines and ensures comparability across subjects [13]. Minor variability may also arise from the use of two different PET/CT scanner models across institutions. Although liver normalization helps mitigate inter-scanner differences, it may not fully eliminate them. We also acknowledge that findings may not generalize to populations with low smoking burden or different metabolic phenotypes. Additionally, while we defined ex-smokers as individuals abstinent for more than six months, the duration of cessation likely influences residual inflammation. A more granular analysis based on years since quitting was not feasible in this retrospective design but would provide valuable insight into the reversibility of smoking-related inflammation.

Future prospective studies should integrate PET findings with biochemical and histological validation and explore therapeutic implications-specifically, whether persistent arterial ^{18}F-FDG uptake in ex-smokers is modifiable through targeted anti-inflammatory interventions or statin therapy. The cellular basis of persistent arterial ^{18}F-FDG uptake may relate to macrophage-driven inflammation, particularly polarization toward pro-inflammatory phenotypes implicated in active atherosclerotic lesions [22].

Statins have demonstrated efficacy in reducing vascular inflammation as assessed by ^{18}F-FDG PET/CT in interventional studies. A recent systematic review and meta-analysis confirmed that statin therapy significantly lowers arterial ^{18}F-FDG uptake, particularly with high-intensity regimens, reinforcing the role of ^{18}F-FDG PET/CT both as a diagnostic biomarker and a tool for monitoring treatment response [23]. These findings highlight a potential window for therapeutic modulation.

In conclusion, ^{18}F-FDG PET/CT can detect modest suppression of mucosal immune activity in smokers and persistent vascular inflammation in ex-smokers. Normalization to liver SUVmax is essential to reveal these effects, especially in metabolically heterogeneous populations. These findings highlight the multifactorial nature of inflammation - shaped not only by smoking status but also by factors such as BMI and metabolic status - that can confound unadjusted analyses. Positron emission tomography/CT with appropriate normalization may serve as a valuable tool for inflammation profiling and cardiovascular risk stratification in individuals with a history of tobacco exposure.

The authors declare that they have no conflicts of interest.

Compliance with Ethical Standards

This study was performed in line with the principles of the Declaration of Helsinki. Approval was granted by the Ethics Committee of the University Hospital of Larissa and the Theageneio Anticancer Centre (16 March 2021 / 17/4/16.03.21).

Bibliography

1. World Health Organization. Tobacco Fact Sheet. Geneva: *WHO;* 2023.
2. Brandtzaeg P. Immunology of tonsils and adenoids. *Int J Pediatr Otorhinolaryngol* 2003; 67(Suppl 1): S69-76.
3. Elisia I, Lam V, Cho B et al. The effect of smoking on chronic inflammation, immune function and blood cell composition. *Sci Rep* 2020; 10: 19480.
4. Libby P. Inflammation in atherosclerosis. *Nature* 2002; 420: 868-74.
5. Kassi E, Pervanidou P, Kaltsas G, Chrousos G. Metabolic syndrome: definitions and controversies. *BMC Med* 2011; 9: 48.
6. Rudd JHF, Myers KS, Bansilal S et al. Atherosclerosis inflammation imaging with FDG PET: carotid, iliac, and femoral uptake vs risk factors. *J Nucl Med* 2008; 49: 871-7.
7. Tarkin JM, Joshi FR, Evans NR et al. Detection of atherosclerotic inflammation by ^{68}Ga-DOTATATE PET compared to ^{18}F-FDG PET imaging. *J Am Coll Cardiol* 2017; 69: 1774-91.
8. Tawakol A, Migrino RQ, Bashian GG et al. In vivo ^{18}F-FDG PET imaging provides a noninvasive measure of carotid plaque inflammation in patients. *J Am Coll Cardiol* 2006; 48: 1818-24.
9. Figueroa AL, Abdelbaky A, Truong QA et al. Measurement of arterial activity on routine ^{18}F-FDG PET/CT improves prediction of future cardiovascular events. *JACC Cardiovasc Imaging* 2013; 6: 1250-9.
10. Rominger A, Saam T, Vogl E et al. ^{18}F-FDG PET/CT identifies patients at risk for future vascular events. *J Nucl Med* 2009; 50: 1611-20.
11. Rudd JH, Warburton EA, Fryer TD et al. Imaging atherosclerotic plaque inflammation with ^{18}F-fluorodeoxyglucose positron emission tomography. *Circulation* 2002; 105: 2708-11.
12. Tatsumi M, Cohade C, Nakamoto Y, Wahl RL. Fluorodeoxyglucose uptake in the aortic wall at PET/CT: possible finding for active atherosclerosis. *Radiology* 2003; 229: 505-10.
13. Boellaard R, Delgado-Bolton R, Oyen WJ et al. ^{18}F-FDG PET/CT: EANM procedure guidelines for tumour imaging. *Eur J Nucl Med Mol Imaging* 2015; 42: 328-54.
14. Lodge MA. Repeatability of SUV in oncologic PET. *J Nucl Med* 2017; 58: 523-32.
15. Mortaz E, Kraneveld AD, Smit JJ et al. Effect of cigarette smoke extract on dendritic cells and their impact on T-cell proliferation. *PLoS One* 2009; 4: e4946.
16. Ridker PM, Everett BM, Thuren T et al. Antiinflammatory therapy with canakinumab for atherosclerotic disease. *N Engl J Med* 2017; 377: 1119-31.

17. Coulson JM, Rudd JHF, Duckers JM et al. Excessive aortic inflammation in chronic obstructive pulmonary disease: an ^{18}F-FDG PET pilot study. *J Nucl Med* 2010; 51: 1357-60.
18. Torigian DA, Green-McKenzie J, Liu X et al. A study of the feasibility of ^{18}F-FDG-PET/CT to systematically detect and quantify differential metabolic effects of chronic tobacco use in organs of the whole body. *Acad Radiol* 2017; 24: 326-36.
19. Hansson GK. Inflammation, atherosclerosis, and coronary artery disease. *N Engl J Med* 2005; 352: 1685-95.
20. Hansson GK, Libby P. The immune response in atherosclerosis: a double-edged sword. *Nat Rev Immunol* 2006; 6: 508-19.
21. van der Valk FM, Verweij SL, Zwinderman K et al. Thresholds for arterial wall inflammation quantified by ^{18}F-FDG PET: implications for vascular risk. *J Am Coll Cardiol* 2016; 67: 1211-21.
22. Stöger JL, Gijbels MJJ, van der Velden S et al. Distribution of macrophage polarization markers in human atherosclerosis. *Atherosclerosis* 2012; 225: 461-8.
23. Pirro M, Simental-Mendia LE, Bianconi V et al. Effect of statin therapy on arterial wall inflammation based on ^{18}F-FDG PET/CT: a systematic review and meta-analysis of interventional studies. *J Clin Med* 2019; 8: 118.